



Superconducting Magnet Division

Magnet Note

Author: W. Fischer, A. Jain, and S. Tepikian

Date: January 5, 2001

Topic No: 600-11 (AM-MD-301)

Topic: Magnet Measuring Results and Techniques

Title: Beam-based Measurements of Persistent Current Decay in RHIC

NOTE: This magnet note is also published as a CAD Note C-A/AP/32, November 21, 2000

M. Anerella	S. Ozaki (c)
A. Blake (c)	B. Parker
J. Cozzolino	S. Peggs
J. Escallier (c)	F. Pilat (c)
G. Ganetis	S. Plate (c)
M. Garber (c)	C. Porretto (c)
A. Ghosh	W. Sampson (c)
R. Gupta	J. Schmalzle (c)
H. Hahn (c)	J. Sondericker (c)
M. Harrison	S. Tepikian (c)
J. Herrera	R. Thomas (c)
A. Jain	D. Trbojevic (c)
P. Joshi (c)	P. Wanderer
S. Kahn	J. Wei
W. Louie (c)	T. Wild (c)
G. Morgan (c)	E. Willen
J. Muratore (c)	

Beam-based Measurements of Persistent Current Decay in RHIC

W. Fischer, A. Jain and S. Tepikian

November 21, 2000

Abstract

The two RHIC rings are equipped with superconducting dipole magnets. At injection, induced persistent currents in these magnets lead to a sextupole component. As the persistent currents decay with time, the horizontal and vertical chromaticities change. From magnet measurements of persistent current decays, chromaticity changes in the machine are estimated and compared with chromaticity measurements.

1 Introduction

Persistent currents are eddy currents that are induced in the filaments of superconducting magnets through a change in the magnetic field. They lead to field distortions in the magnets. At a constant field during injection these currents decay with time. Decay rates typically vary from magnet to magnet and depend on the magnetic field history as well as on cable properties [1].

The magnetic field errors inside long straight magnets can be described through multipole coefficients according to

$$B_y + iB_x = B_{ref} \sum_{n=0}^{\infty} (b_n + ia_n) \left(\frac{x + iy}{r_0} \right)^n, \quad (1)$$

where B_x and B_y denote the horizontal and vertical magnetic field respectively, B_{ref} a reference field, x and y the horizontal and vertical position, r_0 a reference radius and i the imaginary unit. The reference radius chosen for most of the RHIC magnets is 25 mm. The multipole coefficients b_n denote normal and the coefficients a_n skew components of the field and are quoted in units of 10^{-4} . Persistent currents generate all multipoles which are allowed by coil symmetry, i.e. b_0, b_2, b_4, \dots in dipoles and b_1, b_3, b_5, \dots in quadrupoles.

At injection energy, the sextupole field errors b_2 from persistent currents can be significant due to their size and time-dependence. The chromaticity stemming from persistent currents can surpass the natural chromaticity and its uncorrected change during injection may be unacceptable for operation. Time dependence is not only observable as a slow decay at the injection level but also as a snap-back to the original multipole value when acceleration starts. For the four large hadron machines in existence or under construction, Tab. 1 gives an overview of the effect of persistent currents on the chromaticity

Table 1: Overview of the effect of persistent currents on the chromaticity at injection in various large hadron accelerators [2-7].

	Energy	Natural		Persistent current		Change over	
	range	Chromaticity		Chromaticity		15min*	
	E_{top}/E_{inj}	$\xi_{x,n}$	$\xi_{y,n}$	ξ_{x,b_2}	ξ_{y,b_2}	$\Delta\xi_x$	$\Delta\xi_y$
Tevatron [†]	7	-20	-20	-140	+119	+8	-7
HERA-p	23	-44	-47	-275	+245	+26	-23
RHIC	10	-55	-57	-38	+36	+2	-2
LHC	16	-80	-80	-600	+600	+180	-180

* Uncorrected chromaticity change, starting 2 min after reaching the injection plateau.

[†] Original fixed target configuration.

at injection. For an effective correction of persistent current effects, reproducibility and predictability are important. In this article we compare for both RHIC rings the expected chromaticity changes from magnet measurements with measured chromaticity changes.

In the following we present magnet measurements of persistent current decays, calculations of expected chromaticity changes at injection, and chromaticity measurements as a function of time. During the year 2000 gold run, beam was injected in RHIC at a dipole current of 462 A and ramped to 3169 A for physics stores. At the end of a store the dipole current was ramped down to a park level of 50 A, after a stop at the injection level, and back to the injection level. The ramp rate between the injection and storage level was 25 A/s, between the injection and park level it was 5 A/s. Time-dependent chromaticity measurements in both the Blue and Yellow ring started 2 min after reaching the injection current and extended over 15 min.

2 Magnet Measurements of Persistent Current Decays

The expected time-dependent chromaticity change can be deduced from two magnet measurements. First, the persistent current decay was measured in 20 magnets at 660 A, a current higher than the injection current of 462 A. Second, the decay was also measured in a single dipole magnet at 470 A.

For the measurement of the decay in the 20 magnets, the current was ramped up to 5000 A and down to 25 A at a rate of 80 A/s, and then back up to 660 A at a rate of 16 A/s. Fig. 1 shows the change in b_2 in these magnets after reaching 660 A on a linear time scale in part (a) and on a logarithmic time scale in part (b).

To describe the measured data, they were fitted to two functions. First, a logarithmic time dependence was assumed according to

$$b_2 = c_0 + c_1 \log_{10}(t/\tau_1) \quad \text{with} \quad \tau_1 = 1 \text{ s}, \quad (2)$$

Such a time-dependence is characteristic of a relaxation process, namely the flux creep phenomenon in hard superconductors. The HERA magnets could be characterized this

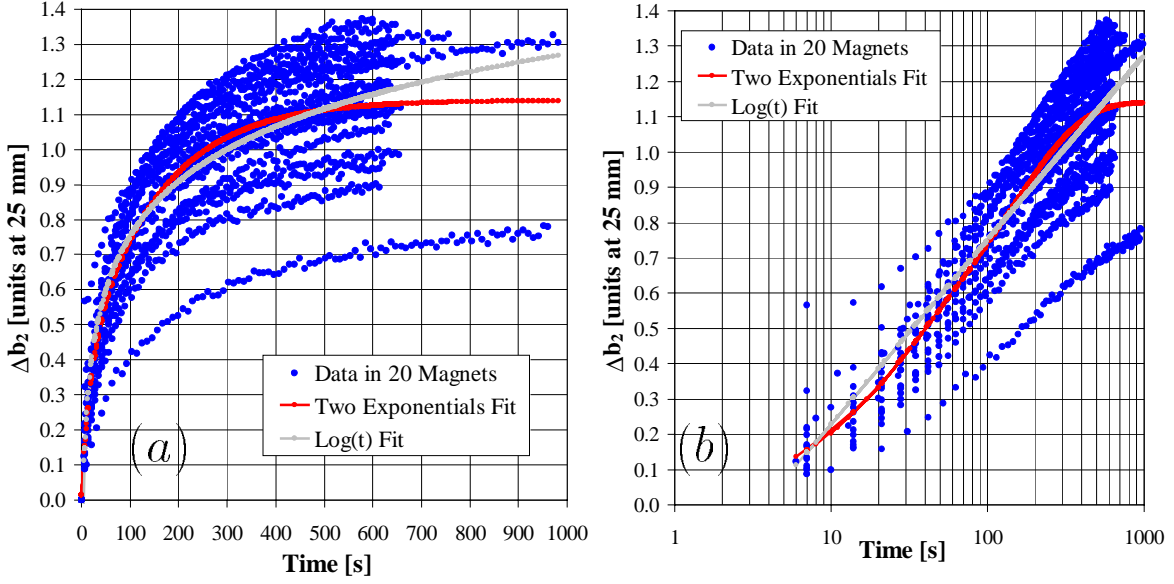


Figure 1: Time-dependent change of the sextupole coefficient in 20 RHIC dipoles at 660 A. Part (a) shows the dependence on a linear time scale, part (b) on a logarithmic time scale.

way [8]. Another fit for the RHIC magnets can be obtained with two superimposed exponentially decaying terms according to

$$b_2 = c_0 + c_1 e^{-t/\tau_1} + c_2 e^{-t/\tau_2}. \quad (3)$$

An exponential decay is expected when the eddy current loops are partly superconductive and partly resistive. Such loops could be between filaments or strands. Eddy current loops between filaments, however, should have decay constants of less than a second and should be irrelevant on the time-scale of our investigation [8]. In Tab. 2 the fitted coefficients are shown for both functions together with the change in b_2 over 15 min, starting 2 min after reaching 660 A. The fitted functions are also shown in Fig. 1. The fit with Eq. (2) overestimates the decay while the fit (3) underestimates the decay. The fitted time constants in Eq. (3) are not very robust, i.e. small changes in the experimental data can change these time constants considerably.

Since the persistent currents are approximately independent of the main field at transport currents well below the critical current, the coefficients c_0 , c_1 and c_2 in Eqs. (2) and (3) can be scaled with the reference field. For 462 A the average dipole field is 0.3260 T, for 660 A the field is 0.4663 T. The result of scaling is also shown in Tab. 2. However, measurements in a single LHC dipole prototype, built at BNL, seem to indicate that such a simple scaling tends to overestimate the persistent current decay when scaled from higher to lower current. Furthermore, the magnets were cycled to 5000 A, higher than the 3169 A used in the beam-based measurements. Measurements in a single RHIC dipole show that the persistent currents decay faster when the magnet is cycled to a higher current [9].

Table 2: Time-decay coefficients from magnet measurements. Coefficients for the logarithmic fit are according to Eq. (2), coefficients for the two exponentials fit are according to Eq. (3). The change in b_2 is computed from 2 min to 17 min with the fitted functions. b_2 and the coefficients c_1, c_2 are quoted in units of 10^{-4} .

Measurement	Logarithmic fit		Two exponentials fit				
	c_1 [1]	Δb_2 [10^{-4}]	c_1 [1]	τ_1 [s]	c_2 [1]	τ_2 [s]	Δb_2 [10^{-4}]
20 magnets at 660 A, average	+0.52	0.49	-0.35	19.7	-0.78	151.0	0.35
20 magnets scaled to 462 A	+0.75	0.69	-0.50	19.7	-1.11	151.0	0.50
1 magnet at 470 A	+0.85	0.79	-1.42	49.4	-0.43	458.0	0.41

Extensive measurements of dynamic effects, including the sextupole time decay and snap-back, have been carried out with a single dipole using a fast measuring coil system that rotates with a period 0.66 seconds. A detailed report summarizes all these data [9].

Fig. 2 shows the sextupole time decay at 470A, after cycling the magnet to 3500 A and down to 25 A before bringing it to the injection level. The ramp rate during the cycling was 60 A/s. The time $t = 0$ is chosen to be the moment when the power supply current reaches 450 A. Part (a) shows b_2 on linear time scale, part (b) on a logarithmic time scale. It is evident that a simple linear relation between b_2 and $\log(t)$ is not followed by the data over the entire range. The result of fitting these data to the functions (2) and (3) are also shown in Tab. 2.

For beam based measurements, a time interval of 15 min, starting at 2 min, was covered. This lies partially outside the time interval of the magnet measurements. However, the changes beyond 600 seconds are small. Based on the available data and the fits given by Eqs. (2) and (3) b_2 should not change by more than 0.07 units between 600 seconds and 1020 seconds.

The expected change in b_2 from the scaled measurements of the 20 magnets at 660 A differs from the expected change in b_2 from the single magnet measurement at 470 A by some 20%. However, as Fig. 1 shows, individual magnets can differ in their behavior significantly from each other. The change in the sextupole coefficient from 150 seconds to 600 seconds ranged from 0.15 to 0.36 units, with a mean of 0.28 units and a standard deviation of 0.05 units. We will therefore use the scaled measurement of the 20 magnets for an estimate of the expected chromaticity change.

The dependence of the persistent current decay on the ramp rate has been measured in a LHC prototype magnet. This magnet uses the same coil design as the RHIC dipoles, but is a twin aperture magnet with a different yoke design. The superconductor is also different from the RHIC conductor. For the LHC prototype the difference in the fit parameters c_0, c_1, c_2 and τ_1, τ_2 in Eqs. (2) and (3) for ramp rates of 25 A/s and 50 A/s does not exceed 9%. We therefore disregard this effect for the RHIC magnets.

Magnet measurements of persistent current decays were also done for the Tevatron (see Ref. [2]), HERA (Refs. [10, 11]) and the LHC (Refs. [12–14]).

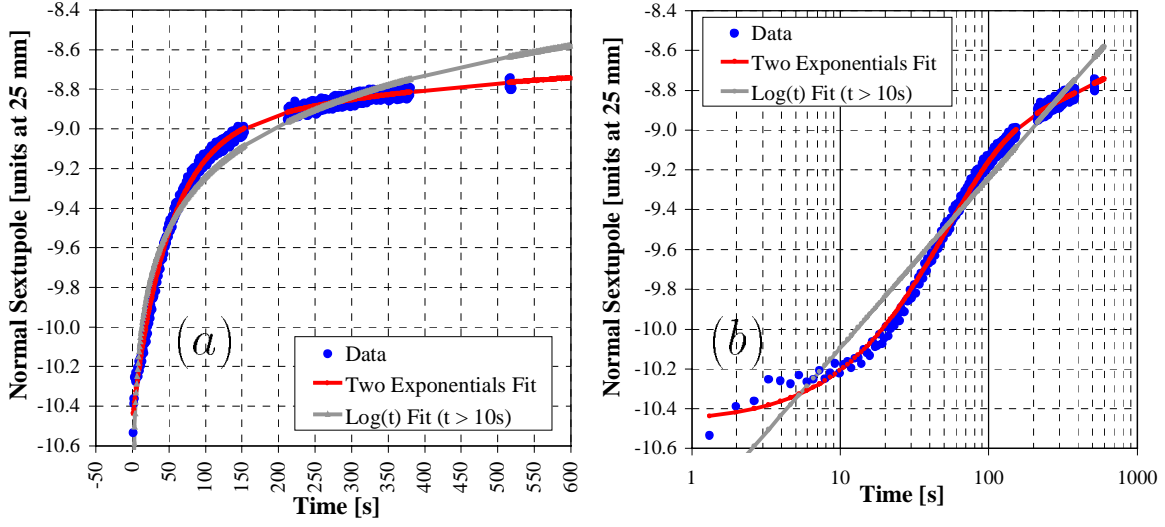


Figure 2: Time-dependent sextupole coefficient in a single RHIC dipole at 470A. Part (a) shows the dependence on a linear time scale, part (b) on a logarithmic time scale.

3 Expected Chromaticity Change From Persistent Current Decay

In this section we compute the expected chromaticity change from the magnet measurements shown in Sec. 2. We will make an analytical estimate and use two optics programs for this purpose. An overview of RHIC is given in Ref. [15].

3.1 Analytical Estimate

We use as definition for the chromaticity

$$\xi_{x,y} = \frac{\Delta Q_{x,y}}{\Delta p/p} \quad (4)$$

where $Q_{x,y}$ are the transverse tunes and $\Delta p/p$ is the relative momentum deviation. The change of chromaticity $\Delta \xi_{x,y}$ associated with the change of the sextupole component Δb_2 can be computed as (see for example Refs. [16, 17])

$$\Delta \xi_{x,y} = \pm \frac{1}{2\pi} \frac{1}{(B\rho)} \oint \beta_{x,y}(s) \frac{B_{ref} \Delta b_2(s)}{r_0^2} \eta_x(s) ds. \quad (5)$$

where $\beta_{x,y}$ is the lattice beta function and η_x the dispersion. B_{ref} may be different from the B in the rigidity ($B\rho$). Assuming sextupole errors only in dipoles Eq. (5) can be written as

$$\Delta \xi_{x,y} = \pm \frac{1}{2\pi} \frac{1}{(B\rho)} \frac{B_{ref} \Delta b_2}{r_0^2} N I_{x,y} \quad (6)$$

where N denotes the number of dipoles and the integrals

$$I_{x,y} = \int_{l_1}^{l_2} \beta_{x,y}(s) \eta_x(s) ds \quad (7)$$

extends over a dipole in a FODO cell. We only consider dipoles in FODO cells. With optics programs it can be determined that the contributions from the interaction regions is only $\Delta\xi_{x,y} = 0.1 \times \Delta b_{2,IR}$, which is small compared with the whole machine (see Tab. 1). This is due to the fact that the DX (beam separators) and D0 magnets on both sides of an interaction region cancel each other and the dispersion in the remaining interaction region dipoles is small.

For simplicity we assume that the FODO cells of length L_p have equal phase advance μ in both planes and a bending angle ϕ for the whole cell. The integrals $I_{x,y}$ can be computed using a thin-lens approximation as [18]

$$I_x = \int_{l_1}^{l_2} ds \left[\beta^+ - 2s \frac{1 + \sin \frac{\mu}{2}}{\cos \frac{\mu}{2}} + 4s^2 \frac{\tan \frac{\mu}{2}}{L_p} \right] \cdot \left[\eta^+ \left(1 - 2s \frac{\sin \frac{\mu}{2}}{L_p} \right) + s^2 \frac{\phi}{2L_p} \right] \quad (8)$$

and

$$I_y = \int_{l_1}^{l_2} ds \left[\beta^+ - 2 \left(\frac{L_p}{2} - s \right) \frac{1 + \sin \frac{\mu}{2}}{\cos \frac{\mu}{2}} + 4 \left(\frac{L_p}{2} - s \right)^2 \frac{\tan \frac{\mu}{2}}{L_p} \right] \cdot \left[\eta^+ \left(1 - 2s \frac{\sin \frac{\mu}{2}}{L_p} \right) + s^2 \frac{\phi}{2L_p} \right]. \quad (9)$$

The maximum beta function β^+ and dispersion η^+ of the cell are given by [18]

$$\beta^+ = \frac{L_p(1 + \sin \frac{\mu}{2})}{\sin \mu} \quad \text{and} \quad \eta^+ = \frac{L_p \phi (1 + \frac{1}{2} \sin \frac{\mu}{2})}{4 \sin^2 \frac{\mu}{2}}. \quad (10)$$

For RHIC at injection we have $(B\rho) = 79.0$ Tm, $B_{ref} = 0.326$ T, $r_0 = 25$ mm, $N = 144$, $l_1 = 2.5$ m, $l_2 = 12$ m, $L_p = 29.6$ m, $\mu = 1.41$ rad, and $\phi = 77.8$ mrad. Substituting everything in Eq. (6) and solving the integrals $I_{x,y}$ numerically we obtain

$$\Delta\xi_x = 4.9 \times \Delta b_2 \quad \text{and} \quad \Delta\xi_y = -4.4 \times \Delta b_2. \quad (11)$$

3.2 Estimate from Optics Programs

For RHIC we use two optics programs, MAD [19] for design and Teapot [20] as an online model in operation. In both cases magnetic field errors can be introduced in the lattice. The natural chromaticity and the effect of a sextupole field error in the dipoles was determined and is shown in Tab. 3 together with the analytical estimate.

The analytical estimate and the coefficients determined from MAD agree very well. The Teapot coefficients are slightly different since Teapot uses a single kick approximation for every dipole while the analytical estimate and MAD use a thick lens model. An estimate for the expected difference can be obtained by replacing the integrals $I_{x,y}$ in Eq. (6) by the product $\beta_{x,y}(\frac{l_1+l_2}{2})\eta_x(\frac{l_1+l_2}{2})(l_2 - l_1)$ which uses only the function values in the center of the dipole. A difference of $0.4 \times \Delta b_2$ is obtained which explains most of the difference between the MAD and Teapot coefficients.

Table 3: The effect of a change in the sextupole component on the chromaticity from an analytical estimate, MAD and Teapot. b_2 is given in units of 10^{-4} at a reference radius of $r_0 = 25\text{mm}$.

	Natural		Chromaticity due	
	Chromaticity		to b_2 in dipoles	
	$\xi_{x,n}$	$\xi_{y,n}$	ξ_{x,b_2}	ξ_{y,b_2}
Analytical	—	—	$+4.9 \times b_2$	$-4.4 \times b_2$
MAD	-54.9	-56.5	$+4.9 \times b_2$	$-4.3 \times b_2$
Teapot	-54.7	-56.6	$+4.2 \times b_2$	$-4.0 \times b_2$

4 Measurements of the Time-dependent Chromaticity

The chromaticity was determined by measuring the tune at different average radii and therefore momenta. The tune was obtained from the Fourier transforms of transverse beam oscillations over 512 turns after the beam was excited with a single small kick [21]. The momentum was changed by $\Delta p/p = \pm 0.0017$. The chromaticity was measured every 16 seconds beginning 2 minutes after reaching the injection plateau. Measurements extended over 15 minutes. Both the Blue and the Yellow ring were measured in gold operation. In Figs. 3 and 4 the results of the time-dependent chromaticity measurements are shown on a linear and logarithmic time scale respectively.

Since the chromaticity change is proportional to the change in the sextupole coefficient b_2 (see Eq. (5)), we attempt to fit the chromaticity to two functions equivalent to Eq. (2) and Eq. (3). These are

$$\xi_{x,y} = \bar{c}_0 + \bar{c}_1 \log_{10}(t/\bar{\tau}_1) \quad \text{with} \quad \bar{\tau}_1 = 1 \text{ s}, \quad (12)$$

and

$$\xi_{x,y} = \bar{c}_0 + \bar{c}_1 e^{-t/\bar{\tau}_1} + \bar{c}_2 e^{-t/\bar{\tau}_2}. \quad (13)$$

The experimental data make a fit to five parameters in Eq. (13) difficult. Furthermore the fast decaying component in Eq. (13) has largely decayed when the beam-based measurements start (compare with Tab. 2). We therefore set $\bar{c}_1 = 0$ and perform only a three parameter fit. The results are shown in Tab. 4 along with the change in chromaticity over a 15 min interval starting 2 min after reaching the injection level.

Tab. 4 also shows the chromaticity change expected from both magnet measurements, the scaled measurement of the 20 magnets and the single magnet measurement. The beam-based measurements agree better with the single magnet measurement than with the scaled measurement of the 20 magnets. The coefficient κ in Tab. 4 gives the deviation of the chromaticity measurement to the expectation from the single magnet measurement. For the exponential fit, κ ranges from -2% to 26% with an average of 0%. The single magnet is a good representative for the average machine. The difference between expected and measured chromaticity change reaches is up to 50% when the measurement of the 20 magnets and the logarithmic fit is used.

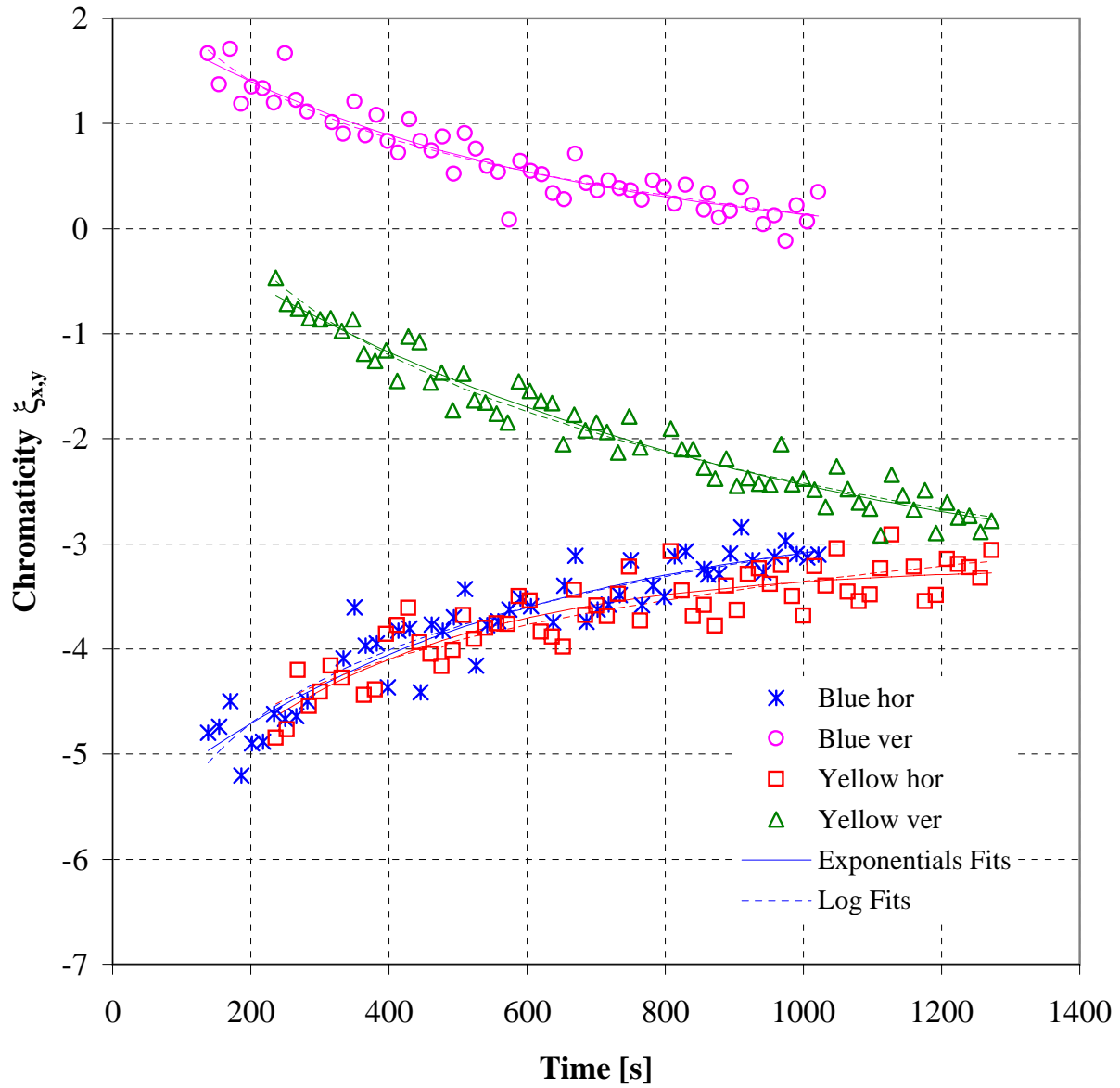


Figure 3: Measured chromaticity in the two RHIC rings on a linear time scale.

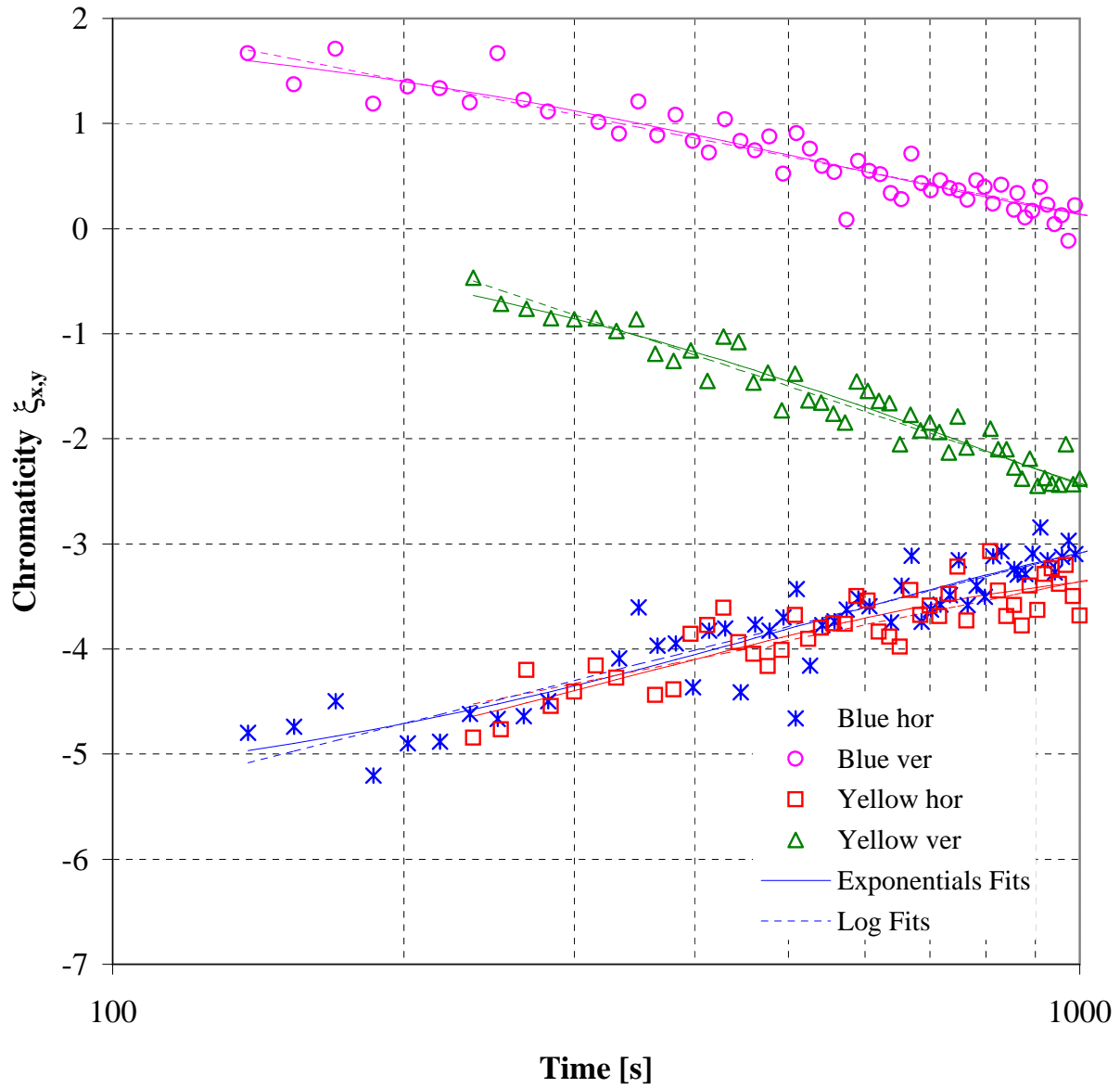


Figure 4: Measured chromaticity in the two RHIC rings on a logarithmic time scale.

Table 4: Chromaticity time-decay coefficients from magnet and beam-based measurements. Coefficients for the logarithmic fit are according to Eq. (12), coefficients for the two exponentials fit are according to Eq. (13). The change in $\xi_{x,y}$ is computed from 2 min to 17 min with the fitted functions. κ denotes the difference between the beam-based measurements and the expectations from the single magnet measurement at 470 A.

Measurement	Logarithmic fit				Exponentials fit					
	\bar{c}_1 [1]	$\Delta\xi_{x,y}$ [1]	κ [%]		\bar{c}_1 [1]	$\bar{\tau}_1$ [s]	\bar{c}_2 [1]	$\bar{\tau}_2$ [s]	$\Delta\xi_{x,y}$ [1]	κ [%]
Horizontal										
From 20 magnets, 660 A scaled	3.66	3.40			-2.44	19.7	-5.54	151.0	2.46	
From single magnet, 470 A	4.17	3.88			-6.96	49.4	-2.12	458.0	2.02	
Blue ring	2.32	2.16	-44		-	-	-3.04	528.6	1.98	-2
Yellow ring	1.86	1.73	-49		-	-	-2.84	346.0	1.86	-8
Vertical										
From 20 magnets, 660 A scaled	-3.29	-3.05			2.19	19.7	4.89	151.0	-2.21	
From single magnet, 470 A	-3.75	-3.48			6.25	49.4	1.91	458.0	-1.81	
Blue ring	-1.81	-1.68	-52		-	-	2.37	535.4	-1.54	-15
Yellow ring	-3.07	-2.85	-18		-	-	3.97	825.5	-2.28	+26

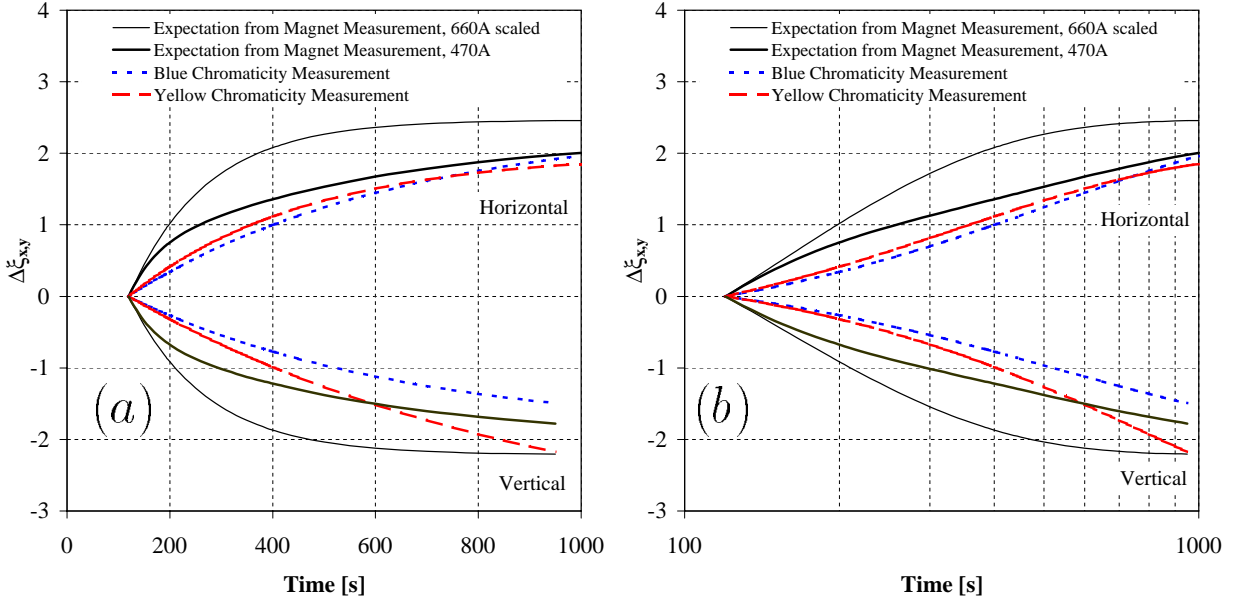


Figure 5: Comparison between chromaticity changes expected from magnet measurements and measured chromaticity changes on a linear time scale in part (a) and logarithmic time scale in part (b). Shown are the exponential fit function.

Fig. 5 also shows the comparison between the expectation from both magnet measurements and the chromaticity measurements, again on a linear and a logarithmic time scale. The single magnet behavior not only agrees much better with the chromaticity measurements at the end of the measurement interval, but also during the interval.

5 Summary

Magnet measurements of persistent current decays in RHIC dipoles show neither a clear logarithmic nor a clear exponential dependence but indicate both components. The relatively small chromaticity changes that can be computed from the measurements of a single magnet agree well with beam-based measurements. The single magnet is a good proxy for both the Blue and Yellow ring with respect to the persistent current decay at injection. The agreement with a scaled measurement of 20 magnets, carried out at a higher current and with a different cycle, is less satisfactory.

6 Acknowledgments

We are thankful to R. Thomas and W. Louie for help with the magnet measurements and to the RHIC operations teams for help during the beam based measurements. We are grateful to A. Drees for support of the tune measurement systems. A special thanks to T. Satogata and J. van Zeijts who supported this study in many ways.

References

- [1] P. Schmüser, “Cos θ Superconducting Magnets”, in “Handbook of Accelerator Physics and Engineering” edited by A.W. Chao and M. Tigner, World Scientific (1999).
- [2] D.A. Herrup, W. Kinney, M.J. Lamm, and A. Mokhtarani, “Compensation of Time-dependent Persistent Current Effects in Superconducting Synchrotrons”, Phys. Rev. E Vol. 49, No. 6 pp. 5660-5567 (1994).
- [3] D. Herrup, private communication (2000).
- [4] B.J. Holzer, “Impact of Persistent Currents on Accelerator Performance”, Part. Acc. Vol. 55 pp. [461-471]/215-225 (1996).
- [5] C. Montag and B. Holzer, “Persistent Current Effects in HERA-p”, proceedings of the US-LHC Collaboration Meeting on Accelerator Physics Experiments for Future Hadron Colliders, BNL (2000).
- [6] O. Brüning, “Accumulation and Ramping in the LHC”, proceedings of Chamonix X, CERN-SL-2000-007 DI (2000).
- [7] L. Bottura, “Dynamic Effects in LHC Magnets”, presentation at the VLHC Annual Meeting, Port Jefferson, New York (2000).
http://magnets.rhic.bnl.gov/vlhc101600/Presentations/Luca_Bottura.pdf
- [8] K.-H. Mess and P. Schmüser, “Superconducting Accelerator Magnets”, CERN Accelerator School on Superconductivity in Particle Accelerators, Hamburg, Germany, 1988, CERN 89-04 (1989).
- [9] A. Jain, G. Ganetis, J. Muratore, R. Thomas and P. Wanderer, “Time Decay, Snap-back and Ramp Rate Effects in RHIC 8 cm Dipoles and Quadrupoles”, Magnet Division Note 593-11 (AM-MD-294), (2000).
<http://magnets.rhic.bnl.gov/publications/documents/FastMeasurements.pdf>
- [10] H. Brück, D. Gall, G. Knies, J. Krzywinski, R. Lange, R. Meinke, H. Preissner, P. Schmüser and Y. Zhao, “Time Dependence of Persistent Current Field Distortions in the Superconducting HERA Magnets”, proceedings of the 1990 European Particle Accelerator Conference, Nice, France (1990).
- [11] H. Brück, D. Gall, J. Krzywinski, R. Lange, R. Meinke, H. Preissner, P. Schmüser and Y. Zhao, “Persistent Current Effects in the Superconducting HERA Magnets and Correction Coils”, proceedings of the 1990 European Particle Accelerator Conference, Nice, France (1990).
- [12] L. Bottura, L. Walckiers, R. Wolf, “Field Errors Decay and ‘Snap-Back’ in LHC Model Dipoles”, IEEE Trans. Appl. Sup., 7(2), 602-605 (1997).

- [13] M. Haverkamp, L. Bottura, M. Schneider, “Studies of Decay and Snapback Effects on LHC Dipole Magnets”, proceedings of the 4th European Conf. on Appl. Superconductivity, Sitges, Spain (1999).
- [14] M. Haverkamp, A. Kuijper, A. den Ouden, B. ten Haken, L. Bottura and H. H. J. ten Kate, “Interaction between Current Imbalance and Magnetization in LHC Cables”, proceedings of the Conf. on Appl. Superconductivity, Virginia Beach, Virginia (2000).
- [15] “RHIC Design Manual”, revision of April 1998.
http://www.rhichome.bnl.gov/NT-share/rhicdm/00_toc1i.htm
- [16] M. Conte, W.W. MacKay, “An Introduction to the Physics of Particle Accelerators”, World Scientific (1991).
- [17] D.A. Edwards and M. Syphers, “Linear Betatron Motion”, in “Handbook of Accelerator Physics and Engineering” edited by A.W. Chao and M. Tigner, World Scientific (1999).
- [18] E. Keil, “Lattices for Collider Storage Rings”, in “Handbook of Accelerator Physics and Engineering” edited by A.W. Chao and M. Tigner, World Scientific (1999).
- [19] H. Grote. F.C. Iselin, “The MAD Program – User’s Reference Manual”, CERN/SL/90-13 (AP) Rev. 5 (1996)
- [20] F. Pilat, S. Tepikian, C. Trahern, S. Tepikian, “ A Model of RHIC Using the Unified Accelerator Libraries”, RHIC/AP/146 (1998).
- [21] P. Cameron, R. Connolly, A. Drees, T. Ryan, H. Schmickler, T. Shea, and D. Trbojevic, “ARTUS: A Rhic TUne monitor System”, BNL RHIC/AP/156 (1998).